A Proposed Ultra High Field RF Coil Design for Axial Human Brain Imaging

T. S. Ibrahim[1,2], and R. Abraham[2]

[1]University of Pittsburgh, Pittsburgh, Pennsylvania, United States, [2]University of Oklahoma, Norman, Oklahoma, United States

Introduction: In this work, we present a numerical design of a new 7T RF head coil, the "Cross-Coax Resonator" (CCR). It is design goal is to produce excellent B_1 field localization and signal strength axially throughout the upper-half of the brain. To demonstrate its capabilities, we numerically compare its performance to one of the most widely used coils in current 7T head imaging the TEM resonator [1]. The comparison is done using the finite difference time domain method, a full wave technique for electromagnetic simulations.

Methods: Figure 1 shows axial and sagittal/coronal cross-sectional views through the CCR. Figure 2 shows a sagittal view of the head loaded in the coil. The coil is comprised of two transverse electromagnetic (TEM) coax elements [2] that intersect at their midpoints. The outer conductors from each coax elements form a hollow cross-shaped structure, which is held in place by dielectric material which surrounds the inner conductors. (Teflon was used as this dielectric filler in the simulations.) The resonance frequency of the coil can be tuned by adjusting the length of these inner conductors.

FDTD grids of both the CCR and a volume 16-element TEM coil were developed and loaded with a detailed human head model. The coils were then excited and tuned for 7 tesla operation (298 MHz). The frequency spectrum of the CCR coil resulting from single-strut excitation is shown in Figure 3. The lower frequency mode is the operational mode, which represents a "decoupled operation" in which the magnetic fields resulting from single strut excitation is primarily polarized in the direction orthogonal to the element orientation. As such, utilizing quadrature excitation leads to excellent circularly polarized magnetic fields through axial planes parallel to plane containing the TEM elements.

Both coils were driven in quadrature excitation, and the B_1^+ fields resulting excitation with 100 W peak power square pulse of width 3 ms and recovery time 300 ms were determined in 14 axial planes (0.8 cm apart) taken through the human head (Figure 4). These represent evenly distributed samples through most of the entire human brain. In addition, a 6.2 cm by 11.4 cm rectangular area centered axially in the brain was then chosen, and the average B_1^+ in this region was determined. (Note that this rectangular region describes most of the brain tissue through axial slices, but does not include the much of the periphery regions of the brain or skull.) Also, the B_1^+ field localization factor defined as the average B_1^+ field inside the rectangular region divided by the average B_1^+ field outside the rectangular region was determined.

Results and Discussion: Figure 5 provides the B_1^+ field distributions through the 14 axial slices taken through the human head. The locations of these slices (positioned in the head) are shown in Figure 3. Figure 6 provides the average B_1^+ field values (in the aforementioned rectangular regions) in axial slices through the human head, and Figure 7 provides the corresponding B_1^+ field localization factors. The analysis shows that the CCR provides higher B_1^+ signal in the specified axial regions throughout the top 5.8 cm of the head compared to the TEM coil. Moreover, it provides considerably higher B_1^+ field localization in the specified rectangular regions through the brain, which has potential to dramatically decrease signal aliasing from surrounding tissue when imaging the specified brain tissue. As such, this coil could provide much higher quality axial images of the upper half of the brain volume than what is currently possible with conventional head volume coils.

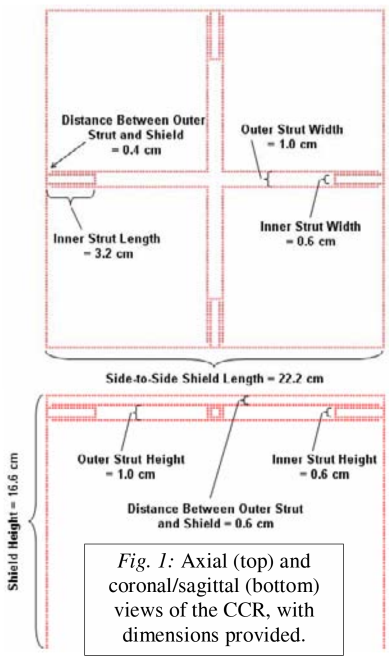

Fig. 1: Axial (top) and coronal/sagittal (bottom) views of the CCR, with dimensions provided.

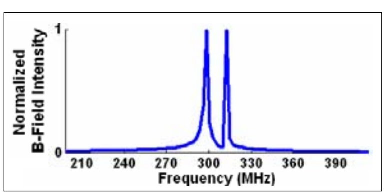

Fig. 3: Frequency spectrum of CCR tuned to 7 Tesla.

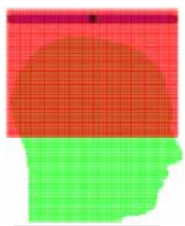

Fig. 2: Sagittal view of CCR loaded with human head

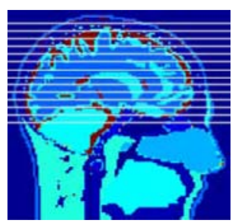

Fig. 4: Sag. view of head showing the locations of the slices shown in Fig 5.

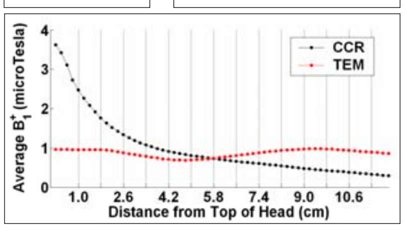

Fig. 6: B_1^+ localization factor in axial slices through the human head.

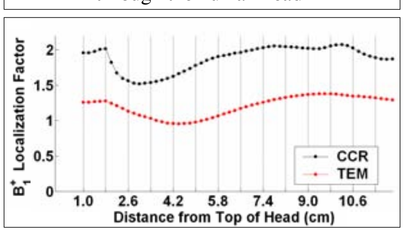

Fig. 7: Average B_1^+ field in axial slices through the human head.

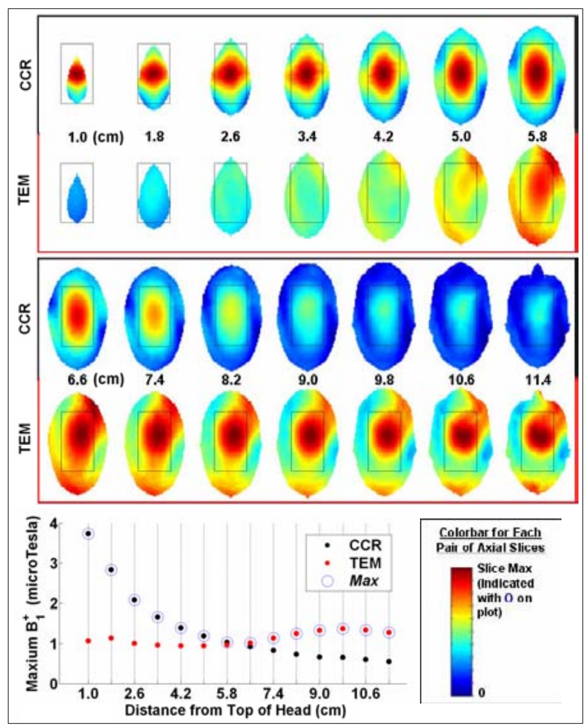

Fig. 5: B_1^+ field distributions in axial slices through the head. The numbers between each pair of slices designate the distance from the top of the head the slices are located (in cm). Every pair of slices has its own colorbar, ranging from 0 to the maximum B_1^+ field value in both slices. These maximum values are provided in the graph. The specified rectangular regions are used to calculate the B_1^+ average values and localization factors in Figs. 6 and 7.

References:

[1] Vaughan, J. T., et al. *Magn. Reson. Med.,* vol 32, pp 206-218, 1994.
[2] Roschmann, P. K., inventor. *U.S. Patent, assignee*. 4,746,866. 1998.